DEUTSCHES ELEKTRONEN-SYNCHROTRON DESY

DESY SR-75/12
September 1975

Excitons in Pure and Doped Solid Neon

by

D. Pudewill
II. Institut für Experimentalphysik der Universität Hamburg

F.-J. Himpsel, V. Saile, N. Schwentner, and M. Skibowski
Sektion Physik, Universität München

E. E. Koch
Deutsches Elektronen-Synchrotron DESY, Hamburg

2 HAMBURG 52 · NOTKESTIEG 1

To be sure that your preprints are promptly included in the
HIGH ENERGY PHYSICS INDEX ,
send them to the following address (if possible by air mail) :

DESY
Bibliothek
2 Hamburg 52
Notkestieg 1
Germany

Excitons in Pure and Doped Solid Neon[≠]

D. Pudewill

II. Institut für Experimentalphysik, Universität Hamburg, 2 Hamburg 50

F.-J. Himpsel, V. Saile, N. Schwentner[+], and M. Skibowski[++]

Sektion Physik, Universität München, 8 München 40

and

E.E. Koch

Deutsches Elektronen-Synchrotron DESY, 2 Hamburg 52

≠ Work supported by Deutsche Forschungsgemeinschaft DFG, Deutsches Elektronen-Synchrotron DESY, and Bundesminsterium für Forschung und Technologie BMFT

+ Now at Christian Albrechts Universität, Kiel

++ On leave at Xerox, Palo Alto Research Center, Palo Alto, California and University of Illinois, Urbana-Champaign, Illinois, USA

submitted to phys.stat.sol. (b)

A comprehensive investigation of the optical excitation of pure solid Ne and of Xe, Kr and Ar impurities in Ne has been carried out in the vacuum ultraviolet using synchrotron radiation. Improved preparation techniques and a new sensitive absorption technique for thin films in a reflection geometry made possible for the first time the observation of exciton series up to n=5. The analysis of the data gave new important information on the energetics of excitons in solid Ne. A new value of 21.69 eV for the band gap energy, the energy levels and binding energies for the excitons in pure and doped solid Ne and reliable values for the central cell correction, which are compared to theoretical predictions, have been derived. Furthermore the oscillator strengths for valence excitons up to n=3 in pure Ne could be determined experimentally and a consistent set of optical constants has been obtained.

Eine ausführliche Untersuchung der optischen Anregungen in reinem Ne und in Ne dotiert mit Xe, Kr und Ar wurde im Vakuum Ultraviolett mit Hilfe der Synchrotronstrahlung durchgeführt. Verbesserte Präparationsbedingungen und eine neue empfindliche Methode zur Absorptionsmessung an dünnen Schichten in einer Reflexionsgeometrie ermöglichte zum erstenmal die Beobachtung von Exzitonenserien bis n=5. Die Auswertung der experimentellen Daten lieferte neue wichtige Informationen über die Energiezustände der Exzitonen. Ein neuer Wert für die Energie der Bandlücke von 21,69 eV, die Energiezustände und Bindungsenergien der Exzitonen in reinem und dotiertem Ne sowie zuverlässige Werte für die Central Cell Correction, die mit theoretischen Vorhersagen verglichen werden, konnten gewonnen werden. Ferner wurden die Oszillatorstärken für Valenzband-Exzitonen bis n=3 in reinem Ne und ein konsistenter Satz optischer Konstanten bestimmt.

1. Introduction

The rare gas solids are important being prototype insulators with Van der Waals binding. They have been widely studied for that reason both theoretically and experimentally over the last years (1). The optical absorption and reflection spectra have been systematically investigated in a large photon energy range covering valence and inner shell excitations, lately by using synchrotron radiation (2). In these large band gap materials the onset of electronic absorption is characterized by a number of narrow lines followed by broader continuum-like structures at higher energies. The excitation energies E_n of the narrow lines have been described in terms of a hydrogenic Wannier series of excitons (3) by

$$E_n = E_G - \frac{B}{n^2} \qquad (1)$$

with E_G gap energy, B binding energy and n principal quantum number. Subsequently the theoretical analysis of the excitonic spectra has been refined, and binding energies and oscillator strengths have been calculated for Xe, Kr and Ar and compared to experimental results (4).

In addition, radiationless electronic energy transfer phenomena from gaseous, liquid and solid rare gases and rare gas mixtures have been investigated by studying the emission of vacuum ultraviolet radiation (5). Recently, also photoemission yield spectroscopy on pure (6-9) and doped (10) rare gas solids provided further interesting information about such processes. Furthermore the first photoelectron energy distribution data (11,12) showing a considerable width of the valence bands have been particularly useful in testing the predictions of various band structure calculations (12,13).

Most of the optical and theoretical studies have been performed on solid Xe, Kr and Ar. Comparatively little is known on solid Ne. This is due to experimental difficulties which are caused by its extremely large band gap (> 21 eV) and its low condens_ation temperature (∿ 5 K). Boursey, Roncin, and Damany (14) have obtained an absorption spectrum of solid thin films of Ne, where an exciton series up to n=3 was observed. Reflection spectroscopy and transmission measurements with synchrotron light by Haensel et al. (15) show an exciton series from which a value for the band gap E_G=21.4 eV was obtained (16). The electron energy loss spectra by Daniels and Krüger (17) and Schmidt (18) using electrons of several 10 keV without monochromatization showed similar, though less clearly resolved structures.

Ar, Kr and Xe impurity states in a Ne matrix have been studied by Baldini (19). Gedanken et al. (20) have extended these experiments to molecular impurity states such as benzene and ethylene in Ne. It was found for all these deep lying impurity states that again the Wannier model provides a good description of the excited impurity energy levels E_n^i:

$$E_n^i = E_G^i - \frac{B^i}{n^2} \qquad (2)$$

where E_G^i is the gap energy and B^i the binding energy for the impurity states. However, the observation of more than two members of a series and therefore also a real test of a hydrogenic behaviour and an accurate determination of E_G^i and B^i were hampered by the limited photon energy range available in Baldini's experiments (19) and by vibrational structure and underlying dissociative continua in the case of molecular impurities (20).

The purpose of this paper is to present new results of a comprehensive investigation of the optical excitation of pure solid Ne and of all the rare

gas impurities in solid Ne. The studies were made possible by application of the synchrotron radiation from DESY and improved preparation techniques of condensed films at low temperature in ultra high vacuum. The band gaps and binding energies for the pure solid and the impurities could be determined much more accurately by studying the reflection dips developing for very thin films on a gold substrate for energies where the reflection and absorption show maxima for thick films. Furthermore the results presented here have also been indispensable for our investigations of the dynamical properties of excitons in solid Ne. In these later experiments, which are described elsewhere (21) , the diffusion and decay of excitons in solid Ne and Ne slightly doped with Xe, Kr and Ar has been studied by photoemission yield spectroscopy.

In the next section details of the experiments will be briefly described. In section 3 we present and discuss the experimental results for pure Ne and for the impurity states Ar, Kr and Xe in solid Ne. The results are summarized in section 4.

2. Experiment

The experiments were performed with the radiation of the DESY electron synchrotron, monochromatized with a normal-incidence monochromator. The resolution was 2 Å over the whole energy range (10 to 30 eV), i.e. 0.1 eV at 25 eV. At the exit arm of the monochromator an ultrahigh vacuum chamber was attached. The experimental arrangement, described in detail elsewhere (22) allows for combined optical and photoemission measurements at pressures lower than 5×10^{-10} Torr.

2.1 Samples

The rare gases from L'Air Liquide and Matheson research, which were used as samples, had a purity of $\geq$99.995 % for Ne, 99.9997 % for Ar, 99.995 % for Kr, and $\geq$99.997 % for Xe. They have been used without further attempts for purification. The sample composition was controlled by mixing the appropriate amounts of the constituents in an ultrahigh vacuum gas handling system at a total pressure of 1000 Torr. The composition of the samples given with the results refers to the relative partial pressures in the gas handling system and thus represents only a lower limit for the impurity concentration, since enrichment during condensation has not been taken into account. As samples thin films were prepared in situ by condensing the gases onto a cooled gold substrate. The low temperatures ($\sim$ 5 K) were obtained with a bakeable liquid He flow cryostat.

2.2 Reflection measurements

Light from the monochromator passing through the exit slit hits the sample under an angle of incidence of 7° with respect to the normal of the sample. The intensity of the reflected light $R(\omega)$ is monitored with an open electrostatic photomultiplier (Johnston MM2). The intensity of the incident light

I_o is measured by the same photomultiplier moved into the incident light beam, when the sample is turned out of the light path. Thus the determination of absolute reflectivities is possible. The relative accuracy within a reflectance spectrum is better than 3 % over the whole range. The absolute values are accurate within 10 %. The absolute values were further checked against the reflectance from the Au substrate which is known from the literature (23).

Generally spectra obtained in this way represent the reflectance from the vacuum - rare gas film - gold substrate combination, as schematically shown in Fig. 1. Only for thick films and those spectral ranges, where the absorption of the rare gas film is so high that the contribution from the Au substrate can be neglected the signal represents the true reflectance of the bulk. Outside this range interference effects are present. However, the systematic variation of the film thickness d allows a clear identication of such interferences. Furthermore, model calculations of the reflectance of the film-substrate combination were carried out (section 3.2) based on the formulae for multilayer systems as described for instance in Ref. (24).

The fact that the neon films are almost perfectly transparent apart from the strong absorption band of the n=1 exciton allows a sort of "modified absorption" measurements in a reflection geometry: The main contribution to the reflectance stems from the Au-substrate rare gas interface. It is attenuated by weak transitions in the rare gas film which are observed as dips in the reflectance. Such excitations with comparatively weak absorption, for which this sensitive technique can be successfully used are the higher members $n \geq 2$ of the exciton series in pure neon (Fig. 3) and the impurity states at low impurity concentration (Figs. 6-9).

2.3 Kramers-Kronig analysis

From the reflectance data the dielectric constant (DK) $\hat{\varepsilon} = \varepsilon_1 + i\varepsilon_2$, where ε_1 and ε_2 are the real and imaginary part of the complex dielectric constant, can be obtained via a Kramers-Kronig analysis [25]. We have performed such an analysis for pure Ne using reflectance data for thick films (d > 4000 Å) and suitable extrapolations. The use of a fast data processing system [26] faciliated the analysis and made possible various checks for internal consistency of the data. For $\hbar\omega \to 0$ we used the static dielectric constant $\varepsilon_o = 1.25$ as calculated by the Clausius-Mossotti formula. For the visible and UV range a low reflectance fitting smoothly to both the $\hbar\omega \to 0$ and the measured 2p-reflectance at higher energies was chosen. Care was taken that the phase Θ of the reflection did not show an unphysical behaviour. For energies from 30 to 400 eV the absorption of solid Ne as obtained by Keitel [27] was used for the determination of the reflectance in this range again via the Kramers Kronig relation. Reflectance spectra from 0 to 400 eV were then constructed by combining the extrapolation to lower energies, the measured reflectance in the 2p-excitation region and the calculated reflectance at higher energies (30 - 400 eV). For energies $\hbar\omega > 400$ eV the extrapolation $R \propto \omega^{-4}$ was used. The final analysis gave the ε_1 and ε_2 spectra presented in Fig. 5.

It is worth noting that the accuracy of the excitation energies for the exciton lines with $n \geq 2$ as quoted with our results is independent from any uncertainty introduced by the Kramers-Kronig analysis, since they could be read directly from the spectra. Further we note, that the accuracy of the present reflectance data in the n=1 exciton range was not sufficient in order to deduce the ratio of the spin 1/2 and spin 3/2 components of this band exactly. In particular the outcome of the Kramers-Kronig analysis depends critically on the depth of the minimum within the reflectance band, which could not even be observed for all samples studied (see Fig. 4).

3. Results and Discussion

3.1 Results for pure Neon

The reflectance of a Ne film with a thickness of d=1300 Å condensed onto a gold substrate is shown in Fig. 2. The dominant maximum at 17.8 eV is associated with the n=1 excitons. In the spectral regions A and C outside the strong reflectance band B of the n=1 exciton maxima and minima caused by interference were observed. By varying the film thickness it was confirmed experimentally that all apparent reflectance peaks in the range A are due to interference. For the range C the change of the spectra with film thickness is shown in Fig. 3. For thin Ne films (d=80 Å) four dips are observed in the otherwise flat spectrum. They are assigned to the n=2, n=3, n=4 and n=5 excitons, respectively. With increasing film thickness these dips turn into small peaks. Even for the thickest film (d=10500 Å) there remains structure between the exciton peaks originating from interference.

In Fig. 4 reflectance spectra are shown for four different film thicknesses in the region of the n=1 exciton. For films 50 Å thick the reflectance band is asymmetric. The full reflectance band is only observed for $d \geq 900$ Å. It is characterized by a maximum reflectance of 60 % at 17.83 eV and a shoulder at around 17.6 eV on the low energy side, which for some samples has been observed as a well separated peak.
The results of the Kramers-Kronig analysis as described in section 2.3 are shown in Fig. 5.

3.2 Discussion for pure solid Neon

The experimentally observed excitation energies in the excitonic region of the spectrum are compiled in Table 1. They are compared to the atomic [28] $2p^6 \rightarrow 2p^5ns,ns'$ and to the molecular [29,30] transition energies involved with

the lowest $2p^6$ electron excitations. As Tanaka and Yoshino (30) have shown the molecular band systems, each representing an electronic transition from the ground state to an upper state, are closely related to one of the excited atomic levels ns,ns'. It has been noted in Ref. (15), that there is also a close relationship between the line positions in gaseous and solid Ne and that a discussion in terms of localized Frenkel excitons would be possible. Inspection of Fig. 4 suggests that the spin orbit splitting could be resolved in the present experiment for the n=1 exciton. It amounts to approximately 0.2 eV as taken from the reflectance spectra thus being close to the gas values of 0.17 eV for the $2p \rightarrow 3s,3s'$ lines.

A comparison to previous absorption measurements on solid Ne (14,15) gives general agreement with the results of Ref. (15). However, the present modified absorption experiment enables us to observe members of the exciton series up to n=5 (see the bottom part of Fig. 3). From the systematic investigation of the thickness dependence as displayed in Fig. 3 it is evident that in the reflection spectrum as reported in Ref. (15) the peak at 20.9 eV is caused by interference and does not correspond to the n=3 exciton. Our results for the impurity excitations for $n \geq 2$ in a Ne matrix which clearly show that the binding energies of the excitons are governed by the host matrix and are independent of the guest atoms (see section 3.3 below), are unequivocally in favour of an assignment in terms of the Wannier model. Furthermore, there arise problems in applying the Frenkel exciton model in describing the s-type final states in the solid, as has been discussed by Rössler (31). Our assignments in Table 1 are therefore given in terms of the Wannier picture. Applying eq. (1) and using values for $n \geq 2$ one obtains an excellent fit of the experimental data to the Wannier series formula (see also Fig. 12) yielding new values of E_G=21.69 eV for the gap

energy and B = 5.24 eV for the binding energy. The values for E_G as reported earlier (15) on the basis of an extrapolation using only the n=2 and n=3 members have been 21.4 and 4.3 respectively. It is interesting to note that the shift ΔE_C = 1.04 eV (central cell correction) of the first exciton in pure Ne from the value predicted by the Wannier model is much larger than the corresponding shifs in the other rare gas solids. ($\Delta E_{C,Ar}$ = 0.19 eV, $\Delta E_{C,Kr}$ = 0.03 eV and $\Delta E_{C,Xe}$ = -0.1 eV (red shift)). Thus the Wannier model has to be modified for the n=1 exciton by the introduction of a large central cell correction. According to the theoretical consideration of Hermanson and Phillips (33) based on pseudopotential theory the central cell correction ΔE_C increases with the exciton binding energy B. This relation is borne out quite clearly by the trends observed for both quantities for all four rare gas solids (see Table 2).

For the evaluation of the reflectance data we have used a simple oscillator model in order to simulate the observed band shape of solid Ne. In the calculations we used the reflection formulas (24) for a package with two plane boundaries and homogeneous dielectric constants (DK) for the thin film and the gold substrate (Fig. 1). The computer program allowed for the variation of the parameters such as the background DK ε_o, the resonance frequencies ω_{ok}, halfwidth Γ_k and strengths of the oscillators f_k, the film thickness and the angle of incidence. For the dielectric constant of Ne a simple oscillator model was used

$$\hat{\varepsilon}(\text{neon}) = \varepsilon_o + \omega_p^2 \sum_{k=1}^{2} \frac{f_k}{\omega^2 - \omega_{ok}^2 + i\omega\Gamma_k} \qquad (3)$$

where $\omega_p = (4\pi ne^2/m)^{1/2}$ is the palsma frequency. Examples for the result of such model calculations are portrayed in Fig. 6 and 7. In both cases the static dielectric constant ε_o = 1.3 was chosen as the background DK. In Fig.

6 calculated normal incidence reflectance spectra are shown in the range of the n=1 exciton for a fixed film thickness d = 500 Å. Two oscillators with resonance frequencies at 17.48 and 17.58 eV having the same oscillator strength $f=f_1=f_2$ and the same halfwidth Γ of 0.05 eV have been assumed. These parameters have been chosen in view of the experimentally determined halfwidth of the corresponding transition in solid Ar of 0.05 eV [34] and the spin orbit splitting of the Ne 2p levels in the gas phase [28,35]. Keeping these parameters fixed the oscillator strength f was varied. As can be seen by comparison with Fig. 2 the calculation with f = 0.11 gives a quite reasonable fit to the experimental data as far as the absolute reflectance (∿60 %), the location of the bands, the peak separation (∿0.18 eV) and the overall width of the reflectance band (∿0.3 eV) are concerned. The result of this fit with both spin components having the same oscillator strength indicates that in solid Ne pure LS-coupling with vanishing spin 3/2 component is not realized. The calculation with f=0.08 for both oscillators results in a reflection band with both the absolute reflectivity and the total band width too small. A spectrum calculated with $f_1=f_2=0.25$ yields a reflection band with a larger absolute reflectance and halfwidth than experimentally observed. We note that the f value for the 3s resonance in the gas phase is f=0.139 [36].

For the range of the n=2 exciton results of our model calculation are shown in Fig. 7. Here the resonance frequencies, halfwidth and oscillator strength of two oscillators each with the same oscillator strength f were kept fixed and the film thickness d was varied. In this way the change from a dip in the reflectance to a small peak with increasing filmthickness is clearly demonstrated. This and a similar fit for the n=3 exciton yield estimates for the oscillator strength of f = 0.021 (n=2) and f = 0.008 (n=3), which correspond to the $1/n^3$ law expected for the oscillator strength for Wannier excitons.

3.3 Results for Xe, Kr and Ar impurities in solid Ne

The reflectance spectra for thin films of neon doped with Xe, Kr and Ar are shown in Figs. 8-11. All spectra show a number of bands of reduced reflectance in the transparent region A of pure Ne (see Fig. 2). Compared to the linewidth of the free gas atoms these apparent absorption bands are fairly broad. In order to obtain qualitative information about the influence of the guest atom concentration on the linewidth we have measured spectra for Xe in Ne for three different concentrations. The results are displayed in Fig. 9. With higher concentration the apparent absorption profile becomes broader on the low energy side and even a splitting of the band into two distinct subbands can be observed for the $\Gamma(3/2)$ n=1 band. This result strongly suggests that for the other impurity spectra with a 1 % impurity concentration broadening of the apparent absorption bands due to formation of molecular impurities is also present.

All the observed bands can be grouped into series. For each impurity these spin orbit split impurity exciton series are indicated on top of the spectrum. The minima not labeled in the figures are caused by interference. The energies and assignments of the impurity absorption, as read from the spectra, are listed in Table 3. The values obtained by Baldini (19) for the lowest members are given for comparison.

3.4 Discussion for Xe, Kr and Ar impurities in solid Ne

The spectra from slightly doped Ne films show similar features as observed for pure rare gas solids: for each impurity two series can be assigned, split by spin orbit interaction, converging to the bottom of the conduction band of the host matrix. For $n \geq 2$ the energies of the series members are almost perfectly described by a Rydberg formula (eq. 2). This is de-

monstrated graphically in Fig. 12 where the excitation energies E_n^i are plotted versus $1/n^2$. Thus from the convergence of these series the gap energies E_G^i of the impurity states as well as the spin orbit splitting of the guest atoms in the Ne matrix can be derived with an accuracy of 0.1 eV (Table 3). The spin orbit splitting is compared with the values for the free atoms and those for the pure solids. Further Fig. 12 shows that the term values $T_n^i = E_g^i - E_n^i$ coincide with those for pure Ne. Deviations are observed only for the n=1 excitations where the electron and hole are fairly localized. This shows the influence of the individual guest atoms: $T_1^{Ne/Ne} = 4.20$ eV, $T_1^{Ar/Ne}(\Gamma 3/2) = 3.64$ eV, $T_1^{Ar/Ne}(\Gamma 1/2) = 3.80$ eV, $T_1^{Kr/Ne}(\Gamma 3/2) = 4.10$ eV and $T_1^{Xe/Ne}(\Gamma 1/2) = 3.86$ eV. It follows that the binding energies B^i determined from excitons $n \geq 2$ excited at the guest atoms reflect the properties of pure Ne (Table 4) and are independent of the individual impurity (Table 2). This observation very strongly supports our interpretation in terms of the Wannier model. Within the effective mass approximation the binding energy B (eq. 1) depends only on the dielectric constant ε and the effective mass m^*

$$B = \frac{m^* e^4}{2\hbar^2 \varepsilon^2} \tag{4}$$

with

$$1/m^* = 1/m_e + 1/m_h \tag{5}$$

where m_e and m_h are the electron and hole masses at the center of the Brillouin zone. At the low concentrations investigated distortions of the host lattice by the impurities can be neglected and for excitons with radii greater than the nearest neighbour distance ($n \geq 2$) ε of pure Ne may be used for the calculation of B^i. Electrons excited at the guest atom move in the conduction bands of the host leading to a common value of m_e whereas the hole will be bound to the guest atom. From eq. 4 and 5 an upper limit of

B^i = 5.8 eV is obtained taking typical values for m_e from bandstructure calculations [37] and a B value of B = 5.24 eV for pure Ne from our experiment, while $1/m_h \cong 0$. In order to determine B^i from the experiment one can use n=2, n=3 and n=4 of the $\Gamma(3/2)$ exciton series of Ar in Ne and Kr in Ne (Table 3). One obtains B^{Ar} = 5.27 eV and B^{Kr} = 5.32 eV (Table 4). The experimental accuracy for the energy positions is approximately 0.05 eV at 20 eV and results in an uncertainty of 0.5 eV for the B^i values. Thus the predictions of the Wannier model for the binding energies of $n \geq 2$ excitons of these deep impurity states in solid Ne are in excellent agreement with our experiment. With ε = 1.25 an electron mass m_e = 0.60 (in units of the free electron mass) was determined. Because of the large values for the hole masses m_h of solid Ne we were not able to resolve a distinct difference in the effective masses when excitons are excited from the valence band of pure Ne or from one of the impurity atoms.

From the coincidence of the T_h^i values for $n \geq 2$ one can calculate the band gap energies E_G^i even for those cases, where a direct observation of higher members of the series is not possible. This leads to the gap energies as given in the third row of Table 4.

In the system Xe in Ne the observation of two series including also higher members allows a correct identification of the first absorption bands observed already by Baldini [19]. In order to obtain convincing assignments fitting into two series it was necessary to change the order n=1(3/2) at 9.08 eV, n=1(1/2) at 11.28 eV and n=2(3/2) at 10.04 eV as given in [19] and the reinterpretation given in [38] to the one shown in Fig. 8 and Table 3.

In this way one also avoids the problem of a spin orbit splitting of 2.2 eV for Xe in Ne which would not be consistent with recent photoelectron energy distribution measurements (12).

Turning now to the energy of the n=1 exciton we observe that the overlap of the lowest excited state with the medium is not sufficiently large to make the approximations valid, which are used in the Wannier scheme. The central cell correction ΔE_C accounts for the deviation of the observed energies from the predicted energies derived from the higher member of the exciton series. The values for ΔE_C determined from our measurements are listed in Table 4 and are plotted versus the binding energy in Fig. 13. The calculated relationship between ΔE_C and B shows a monotonic increase of ΔE_C up to binding energies B = 2.4 eV (33) (see Fig. 13). According to Ref. (20,39) this relationship may be adequately described by a linear dependence

$$\Delta E_C = \alpha + \beta B^i \qquad (6)$$

where the constants α and β are determined by the impurity. Our ΔE_C values of 1.67 eV and 1.47 eV for Xe in Ne are quite lower than the value of 2.34 eV assumed in (20,39). Thus the linear fit does not hold.

4. Summary

Important new information on the excitons in pure and rare gas doped solid neon could be obtained in the present experiments:

(a) a consistent set of optical constants was established for pure solid Ne

(b) the binding energies B^i for the impurity excitations are the same as those for pure Ne for $n \geq 2$ and reflect the properties of the host. The Wannier model provides a satisfactory description for excitons in solid Ne.

(c) on the basis of our new data we could not corroborate a linear dependence of the central cell correction ΔE_C on the binding energies B^i.

(d) The old value for the gap energy for pure Ne has been corrected thanks to the possibility to observe the exciton Wannier series up to n=5. The new value is 21.69 eV.

(e) Comparison with calculations based on a simple oscillator model gave quantitative estimates for the oscillator strength of the n=1,2 and 3 excitons (both spin components included) as $f = 0.22$, $f \simeq 0.042$ and $f \simeq 0.016$ respectively.

(f) The energy levels of the impurity states Ar, Kr and Xe within the band gap have been determined and basic parameters have been derived from this. The influence of the concentration on the line shape has been demonstrated.

Acknowledgment

We would like to thank A. Harmsen for his help in the experiments, J. Jortner for stimulating discussions and comments on the manuscript and W. Steinmann for his stimulating interest and support of this work.

References

1. Rare Gas Solids, edited by M.K. Klein and J.A. Venables, Academic Press, New York, in press
2. For a recent review see B. Sonntag, Optical properties in Ref. 1
3. G. Baldini, Phys.Rev. 128, 1562 (1962)
4. See for instance: U. Rössler and O. Schütz, phys.stat.sol. (b) 56, 483 (1973)
5. For a recent review see: J. Jortner, Electronic Excitations in Molecular Crystals, in: Vacuum Ultraviolet Radiation Physics, edited by. E.E. Koch, R. Haensel, and C. Kunz, Pergamon-Vieweg, Braunschweig 1974, p. 263
6. J.F. O'Brien and K.J. Teegarden, Phys.Rev.Letters 17, 919 (1966)
7. N. Schwentner, M. Skibowski, and W. Steinmann, Phys.Rev. B8, 2965 (1973)
8. E.E. Koch, V. Saile, N. Schwentner, and M. Skibowski, Chem.Phys.Letters 28, 562 (1974)
9. I.T. Steinberger, E. Pantos, and I.H. Munro, Phys.Letters 47A, 299 (1974)
10. Z. Ophir, B. Raz, J. Jortner, V. Saile, N. Schwentner, E.E. Koch, M. Skibowski, and W. Steinmann, J.Chem.Phys. 62, 650 (1975)
11. N. Schwentner, F.-J. Himpsel, E.E. Koch, V. Saile, and M. Skibowski, in Vacuum Ultraviolet Radiation Physics, edited by E.E. Koch, R. Haensel, and C. Kunz, Pergamon-Vieweg, 1974, p. 335
12. N. Schwentner, F.-J. Himpsel, V. Saile, M. Skibowski, W. Steinmann, and E.E. Koch, Phys.Rev. Letters 34, 528 (1975)
13. a) U. Rössler et al., to be published
    b) A.B. Kunz, D.J. Mickish, S.K.V. Mirmira, T. Shima, F.-J. Himpsel, V. Saile, N. Schwentner and E.E. Koch, Solid State Communications, in press.
14. E. Boursey, J.Y. Roncin, and H. Damany, Phys.Rev. Lett. 25, 1279 (1970)
15. R. Haensel, G. Keitel, E.E. Koch, N. Kosuch, and M. Skibowski, Phys.Rev.Lett. 25, 1281 (1970)

16. R. Haensel, E.E. Koch, U. Nielsen, and M. Skibowski, III. Int.Conf. on VUV Radiation Physics, Tokyo 1971, Conference Digest 1aA2-3

17. J. Daniels and P. Krüger, phys.stat.sol. (b) 43, 659 (1971)

18. L. Schmidt, Phys.Letters 36A, 87 (1971)

19. G. Baldini, Phys.Rev. 137 A, 508 (1965)

20. A. Gedanken, B. Raz, and J. Jortner, J.Chem.Phys. 58, 1178 (1973)

21. D. Pudewill, F.-J. Himpsel, V. Saile, N. Schwentner, M. Skibowski, J. Jortner, and E.E. Koch, submitted to J.Chem.Phys.

22. N. Schwentner, E.E. Koch, V. Saile, M. Skibowski, and A. Harmsen, in Vacuum Ultraviolet Radiation Physics, edited by E.E. Koch, R. Haensel, and C. Kunz, Pergamon Vieweg, Braunschweig, 1974, p. 792

23. R.B. Cairns and J.A.R. Samson, J.Opt.Soc.Am. 56, 1568 (1966)

24. S.V. Pepper, J.Opt.Soc.Am. 60, 805 (1970)

25. F. Stern, in Solid State Physics, edited by F. Seitz and D. Turnbull, Academic Press, New York 1963, p. 300

26. R. Klucker and U. Nielsen, Computer Phys. Comm. 6, 187 (1973)

27. G. Keitel, Thesis Univ. Hamburg (1970) DESY Interner Bericht F41-70/7

28. C.E. Moore, Natl.Bur.Stand. (US), Circular No. 467, 1, 76 (1949)

29. J.A.R. Samson, J.Opt.Soc.Am. 55, 935 (1965)

30. Y. Tanaka and K. Yoshino, J.Chem.Phys. 57, 2964 (1972)

31. U. Rössler, Chap. 8 in Ref. 1

32. J. Hermanson, Phys.Rev. 150, 150 (1966)

33. J. Hermanson and J.C. Phillips, Phys.Rev. 150, 652 (1966)

34. A. Harmsen, E.E. Koch, V. Saile, N. Schwentner, and M. Skibowski, in Vacuum Ultraviolet Radiation Physics, edited by E.E. Koch, R. Haensel, and C. Kunz, Pergamon Vieweg, Braunschweig 1974, p. 339

35. D.W. Turner, C. Baker, A.D. Baker, and C.R. Brundle, Molecular Photoelectron Spectroscopy (Wiley, New York, 1970)

36. G. Ligget and J.S. Levinger, J.Opt.Soc.Am. 58, 109 (1968)

37. A.B. Kunz and D.J. Mickish, Phys.Rev. B8, 779 (1973)

38. B. Raz and J. Jortner,Chem.Phys.Letters 9, 222 (1971)

39. A. Gedanken, B. Raz and J. Jortner, Chem.Phys.Letters 14, 172 (1972)

Table 1 Excitation energies in eV in the excitonic region of the spectrum for pure neon. Energies for the atomic and molecular transitions are given for comparison

solid (a)	molecule (b)	gas (c) $2p^6 \rightarrow 2p^5ns$ $(n \geq 3)$
		$^2P_{3/2}$ $^2P_{1/2}$
17.6 sh $\Gamma 3/2$ n=1	16.64 system I	16.67
17.83 $\Gamma 1/2$	16.84 system II	16.84
	19.67 system IV	19.69
20.38 n=2 $\Gamma 3/2$, $\Gamma 1/2$		
	19.76 system V,VI	19.78
	20.55 system X,XI	20.57
21.09 n=3 $\Gamma 3/2$, $\Gamma 1/2$		
	20.63 system XII	20.66
		20.94
21.38 n=4 $\Gamma 3/2$, $\Gamma 1/2$		
		21.04
		21.15
21.50 n=5 $\Gamma 3/2$, $\Gamma 1/2$		
		21.24
		21.56 IP
21.69 E_G		
		21.66 IP

(a) this work, for n=1 maxima of the reflectance are quoted the corresponding peak in ε_2 is at 17.49 eV; for $n \geq 2$ the energies correspond to the observed minima in transmission; E_G gap energy

(b) Y. Tanaka and K. Yoshino (Ref. 30); the assignment of the bands is also taken from Ref. 30 .

(c) C.E. Moore (Ref.28); IP: ionization potential

Table 2 Parameters deduced from the excitation energies for excitons in pure Ne compared to the values obtained for the other rare gas solids (2). E_G gap energy, B binding energy, ΔE_{so} spin orbit splitting, ΔE_c central cell correction, i.e. deviation of the excitation energy for the n=1 state from the value predicted by the Wannier model.
All energies are in eV.

	Ne	Ar	Kr	Xe
E_G	21.69	14.2	11.6	9.3
B	5.24	2.3	1.4	0.8
ΔE_{so}	~0.1	0.2	0.64	1.3
ΔE_c	1.04	0.19	0.03	-0.1 (red shift)

Table 3 Excitation energies E_n in eV for excitons in pure Ne and Ar, Kr and Xe impurity states in a Ne matrix. Numbers in brackets from the work of Baldini (Ref. 14) are given for comparison.

	Ne	Ar in Ne		Kr in Ne		Xe in Ne	
		$\Gamma(3/2)$	$\Gamma(1/2)$	$\Gamma(3/2)$	$\Gamma(1/2)$	$\Gamma(3/2)$	$\Gamma(1/2)$
n=1	17.83[a]	12.59	12.80	10.68	11.29	9.06	10.05
		(12.5)	(12.7)	(10.62)	(11.22)	(9.08)	(10.04)
n=2	20.38	14.97	15.31	13.45	14.06	11.32 (11.28)	12.59
n=3	21.09	15.67	16.04	14.14	-	-	13.32
n=4	21.38	15.90	-	14.55	-	-	-
n=5	21.50	-	-	-	-	-	-
E_G	21.69	16.23	16.60	14.78	-	-	13.91

(a) Maximum of the reflectance band; the maximum of the ε_2-curve is at 17.49 eV.

Table 4 Parameters deduced from the excitation energies for excitons in pure Ne and Ar, Kr and Xe impurity states in a Ne matrix. E_G gap energy, B binding energy, ΔE^i_{so} spin orbit splitting of the impurity levels, ΔE_C central cell correction, i.e. deviation of the excitation energy for the n=1 state from the value predicted by the Wannier model. All energies are in eV.

	Ne	Ar in Ne		Kr in Ne		Xe in Ne	
		$\Gamma(3/2)$	$\Gamma(1/2)$	$\Gamma(3/2)$	$\Gamma(1/2)$	$\Gamma(3/2)$	$\Gamma(1/2)$
E_G	21.69	16.23	16.60	14.78	-	-	13.91
B (±0.1)	5.24	5.27	5.18	5.32	-	-	5.28
$E_G=E_2+\frac{B_{Ne}}{4}$	-	16.28	16.62	14.76	15.37	12.63	13.90
$\Delta E^i_{so}=E_G(1/2)-E_G(3/2)$	-	0.34		0.61		1.27	
ΔE_c (±0.5)	1.04	1.60	1.44	1.14	1.16	1.67	1.47

Figure Captions

Fig. 1 Principle of the reflectance measurement from the rare gas solid - Gold substrate sandwich. I_o incident intensity, I_R reflected intensity, α angle of incidence, d thickness of the rare gas film.

Fig. 2 Reflectance of a Ne film with thickness d = 1300 Å evaporated onto a gold substrate for photon energies 10 to 25 eV. The three ranges A, B and C of the spectrum are discussed in the text.

Fig. 3 Reflectance of Ne films evaporated onto a gold substrate for five different film thicknesses in the range of exciton excitations with $n \geq 2$.

Fig. 4 Reflectance of Ne films evaporated onto a gold substrate for four different film thicknesses in the range of the n=1 exciton.

Fig. 5 Reflectance spectrum of a thick (d>3000 Å) Ne film and dielectric functions deduced from it via Kramers-Kronig analysis (for details see text).

Fig. 6 Model calculation for the n=1 exciton. For a fixed film thickness d = 5000Å the oscillator strength is varied. The parameters used are: resonance frequencies $\hbar\omega$ = 17.48 and 17.58 eV, halfwidth 0.05 eV.

Fig. 7 Model calculation for the thickness dependence of the reflectance of Ne on a gold substrate in the range of the n=2 exciton. The parameters used are: resonance frequencies $\hbar\omega$ = 20.28 and 20.38 eV, halfwidth 0.15 eV, oscillator strength f = 0.036.

Fig. 8 Reflectance of a Ne film doped with ∿1 % Xe with thickness d = 2000 Å evaporated onto a gold substrate. The spin orbit split impurity exciton series is indicated on top of the spectrum.

Fig. 9 Reflectance of Ne films doped with ∿0.1 % (solid line), ∿1 % (dashed line), and ∿5 % (dash-dotted line) Xe respectively evaporated onto a gold substrate in range of the n=1 Xe impurity excitations.

Fig. 10 Reflectance of a Ne film doped with ∿1 % Kr with thickness d = 1700 Å evaporated onto a gold substrate. The spin orbit split impurity exciton series is indicated on top of the spectrum.

Fig. 11 Reflectance of a Ne film doped with ∿1 % Ar with thickness d = 1800 Å. The spin orbit split impurity exciton series is indicated on top of the spectrum.

Fig. 12 Excitation energies of excitons in pure Ne (E_n) and of the impurity states of Ar, Kr, and Xe in a Ne matrix (E_n^i) plotted versus $1/n^2$ according to the Wannier model.

Fig. 13 Central cell correction $\Delta E_C = E_1^{exp} - E_1^{cal}$ for the n=1 impurity state of Xe in various materials versus the exciton binding energy B. The dashed curve is from Ref. [20], the solid curve represents the theoretical calculation [32,33]. The new value for Xe in Ne (this work) is shown.

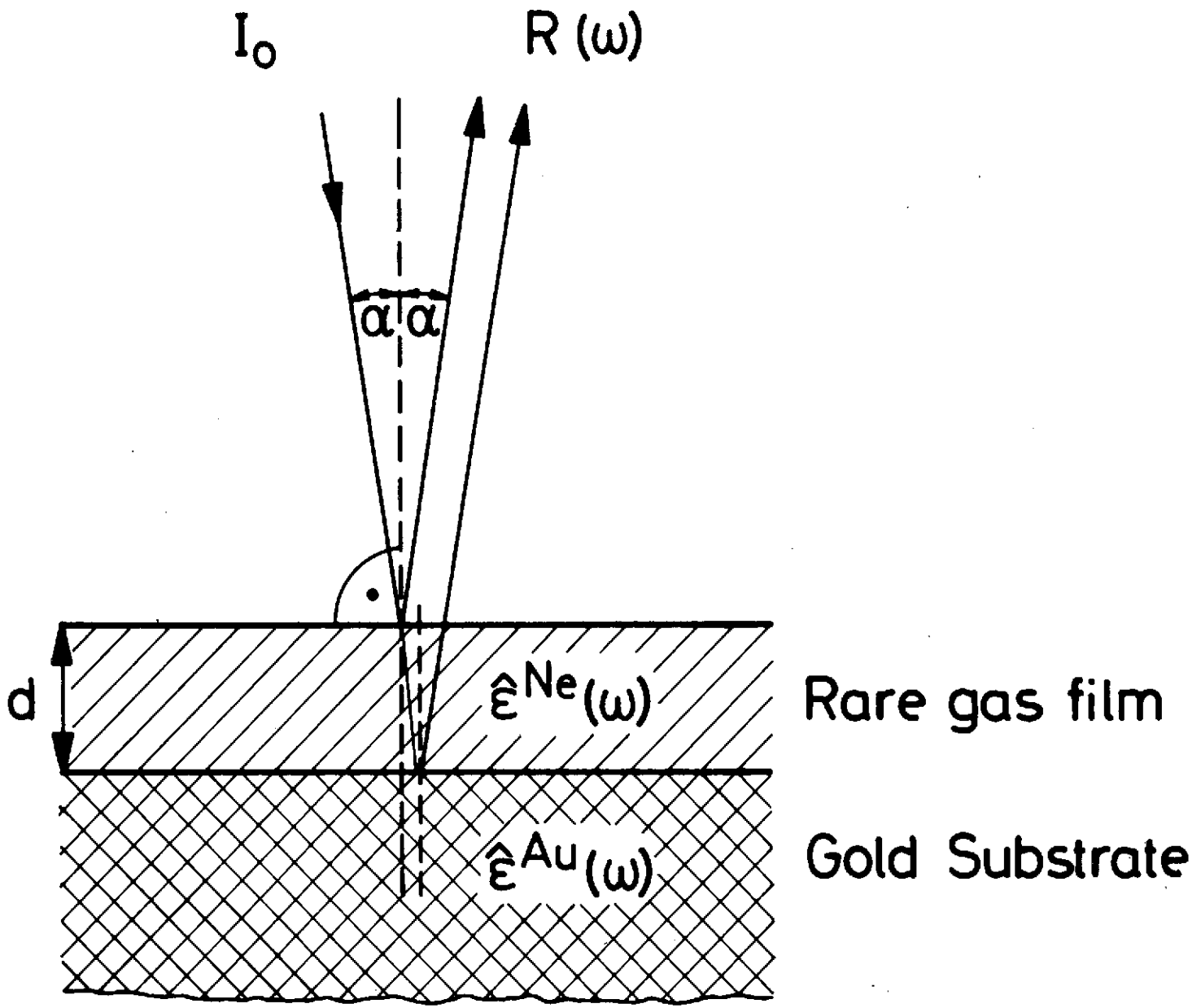
I_o
$R(\omega)$
α α
d
$\hat{\varepsilon}^{Ne}(\omega)$
Rare gas film
$\hat{\varepsilon}^{Au}(\omega)$
Gold Substrate

Fig. 1

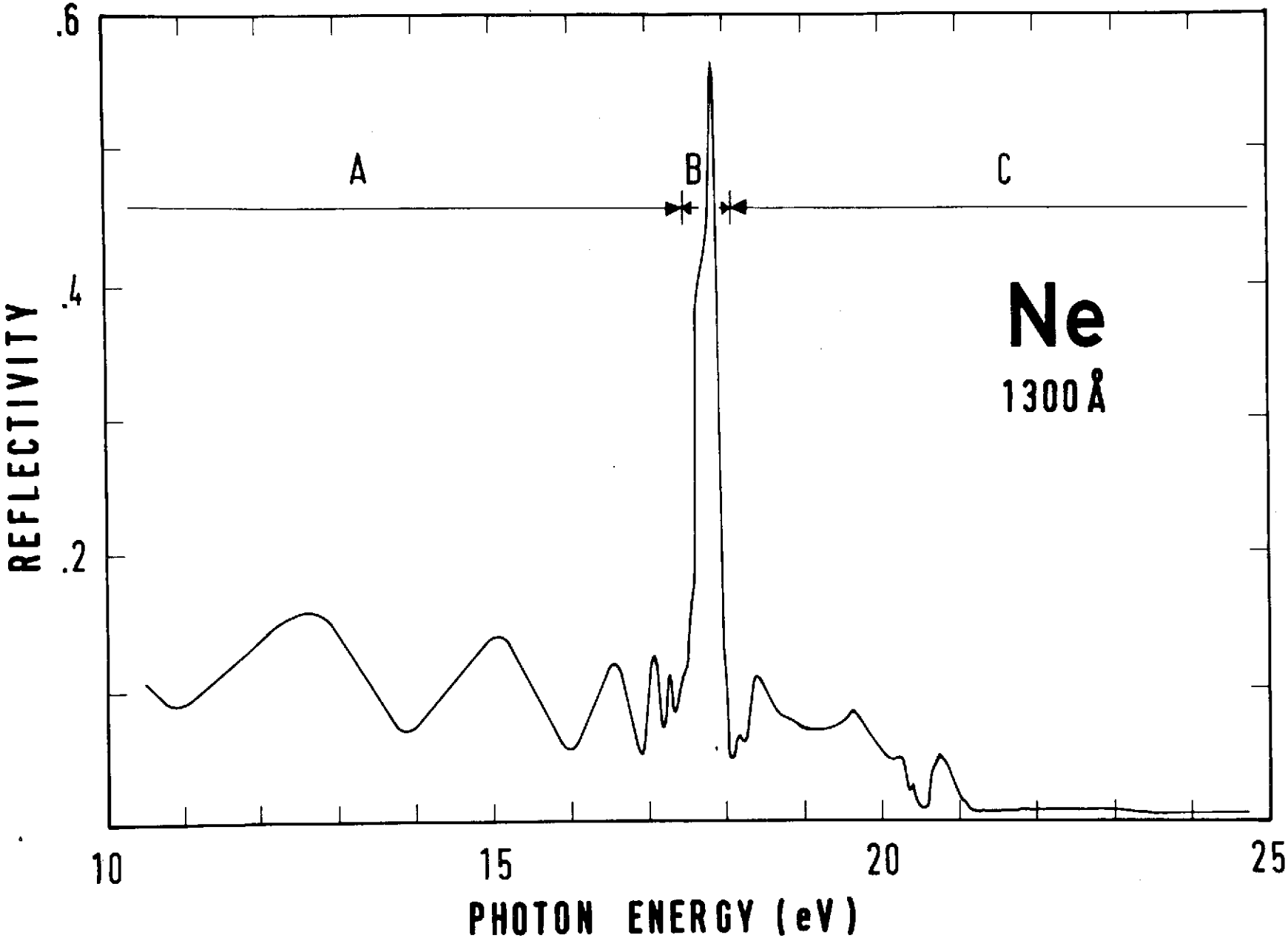

Fig. 2

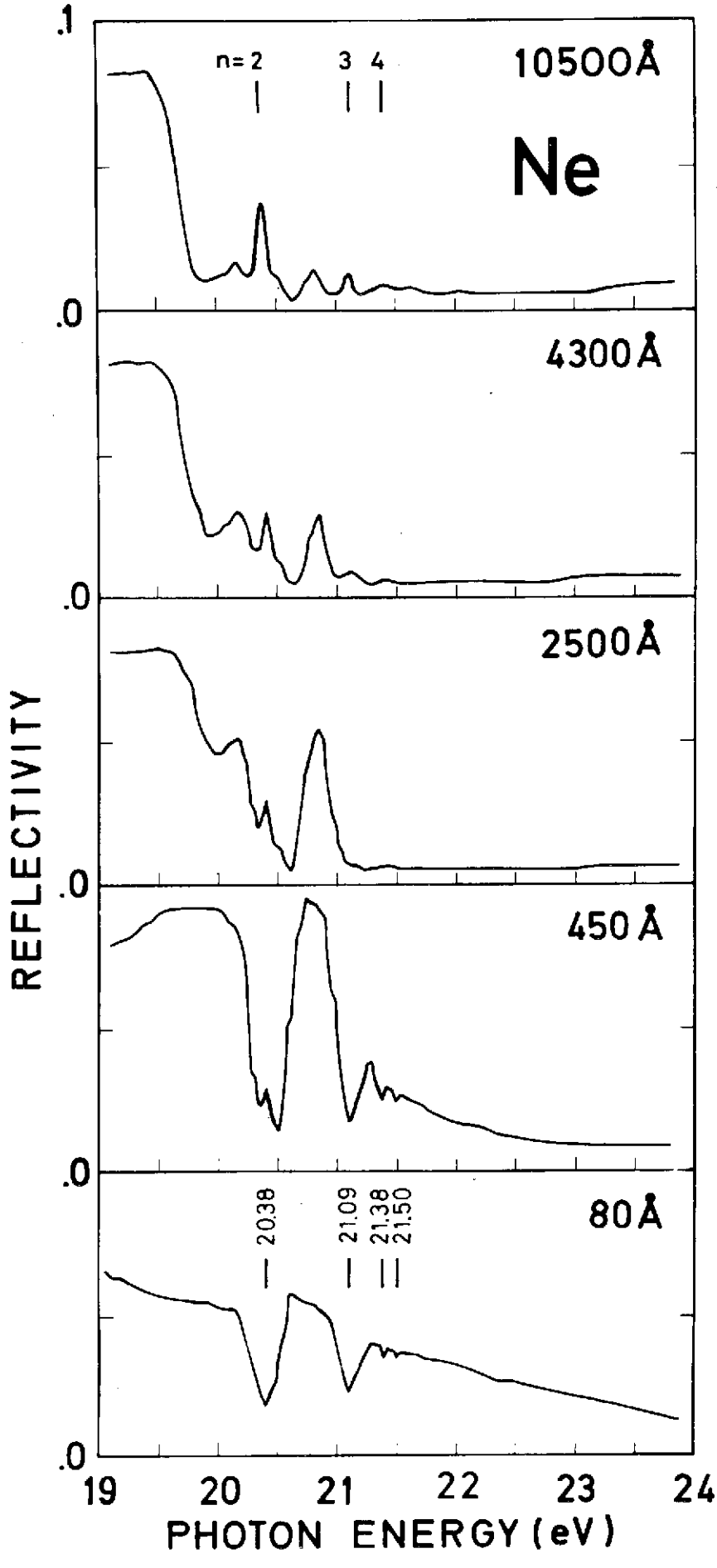
.1
.0
n=2
3
4
10500Å
Ne
4300Å
.0
2500Å
.0
450Å
.0
20.38
21.09
21.38
21.50
80Å
.0
REFLECTIVITY
19
20
21
22
23
24
PHOTON ENERGY (eV)

Fig. 3

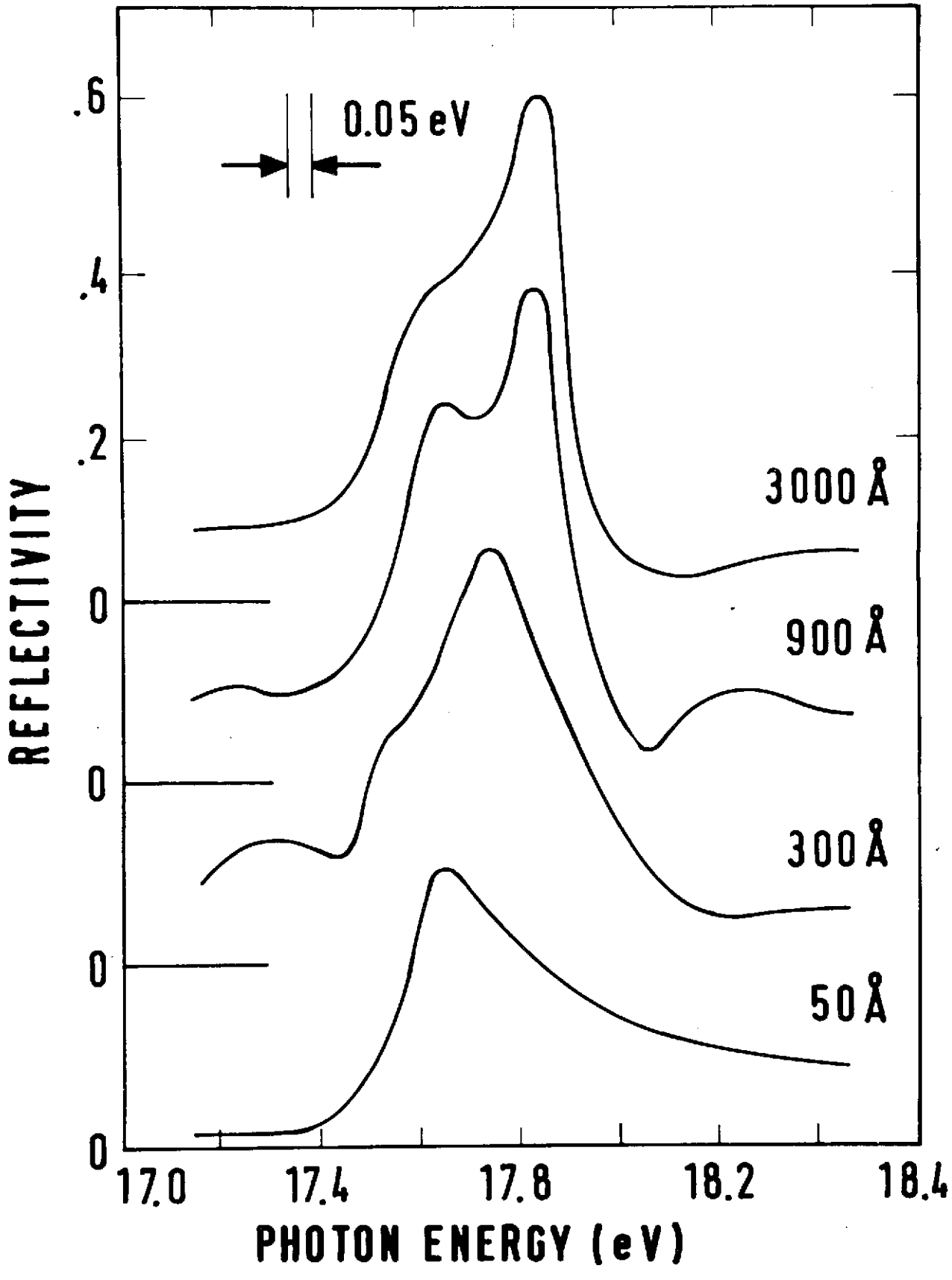
0.05 eV
.6
.4
.2
0
0
0
0
3000 Å
900 Å
300 Å
50 Å
REFLECTIVITY
17.0
17.4
17.8
18.2
18.4
PHOTON ENERGY (eV)

Fig. 4

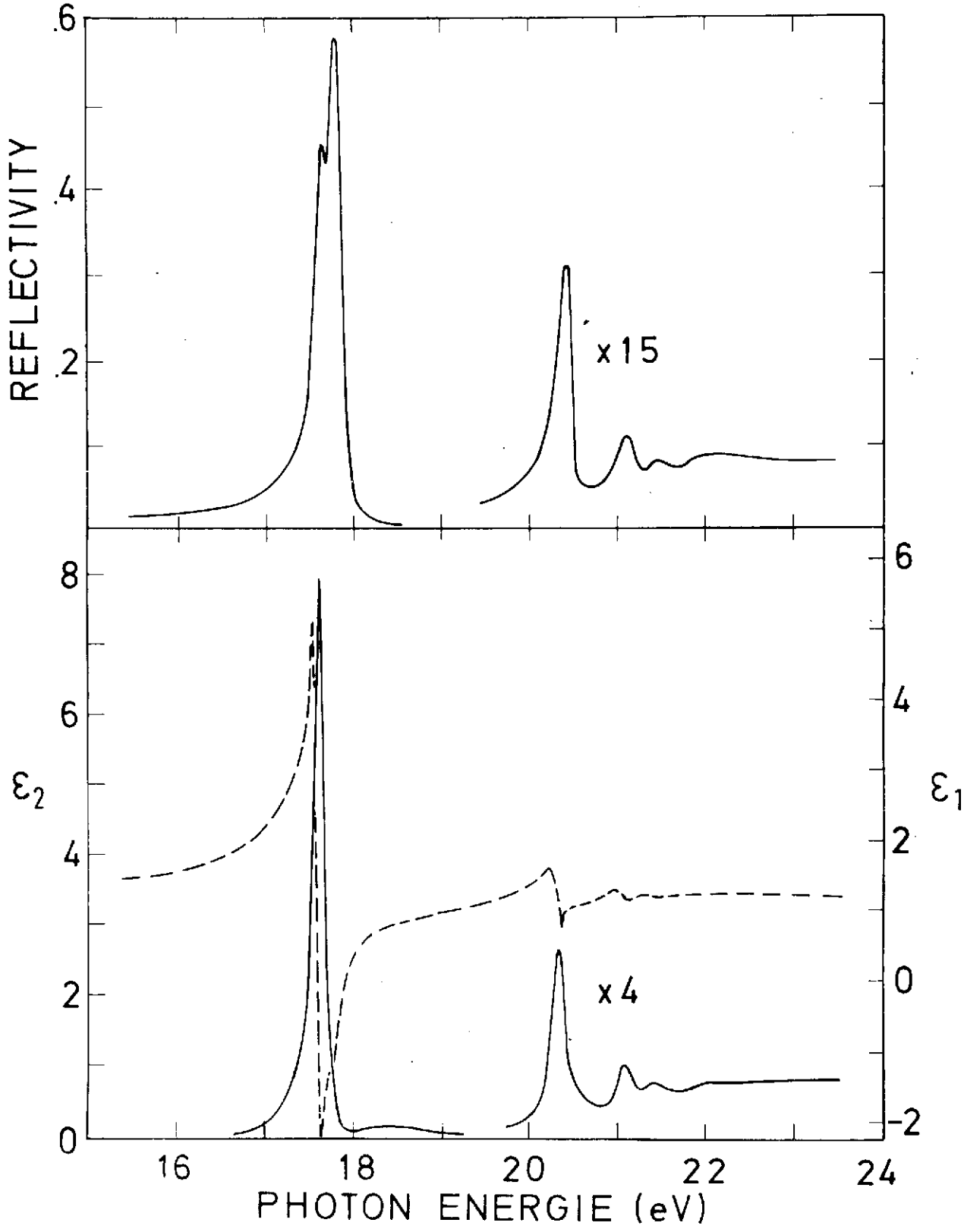
.6
.4
.2
REFLECTIVITY
x15
8
6
4
2
0
ε2
6
4
2
0
-2
ε1
x4
16
18
20
22
24
PHOTON ENERGIE (eV)

Fig. 5

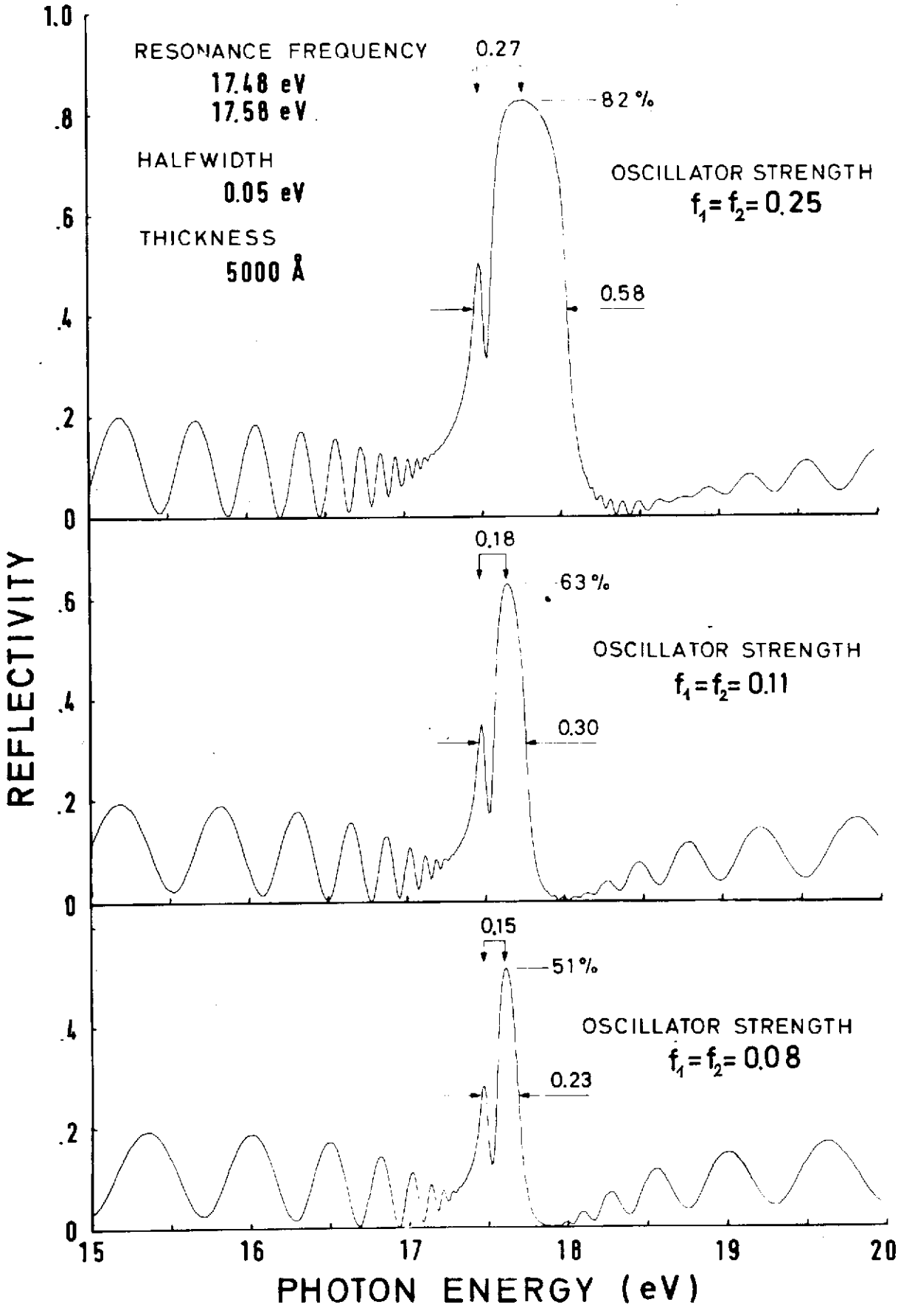
RESONANCE FREQUENCY
17.48 eV
17.58 eV
HALFWIDTH
0.05 eV
THICKNESS
5000 Å
0.27
82 %
OSCILLATOR STRENGTH
$f_1 = f_2 = 0.25$
0.58
0.18
63 %
OSCILLATOR STRENGTH
$f_1 = f_2 = 0.11$
0.30
0.15
51 %
OSCILLATOR STRENGTH
$f_1 = f_2 = 0.08$
0.23
REFLECTIVITY
PHOTON ENERGY (eV)
1.0
.8
.6
.4
.2
0
15
16
17
18
19
20

Fig. 6

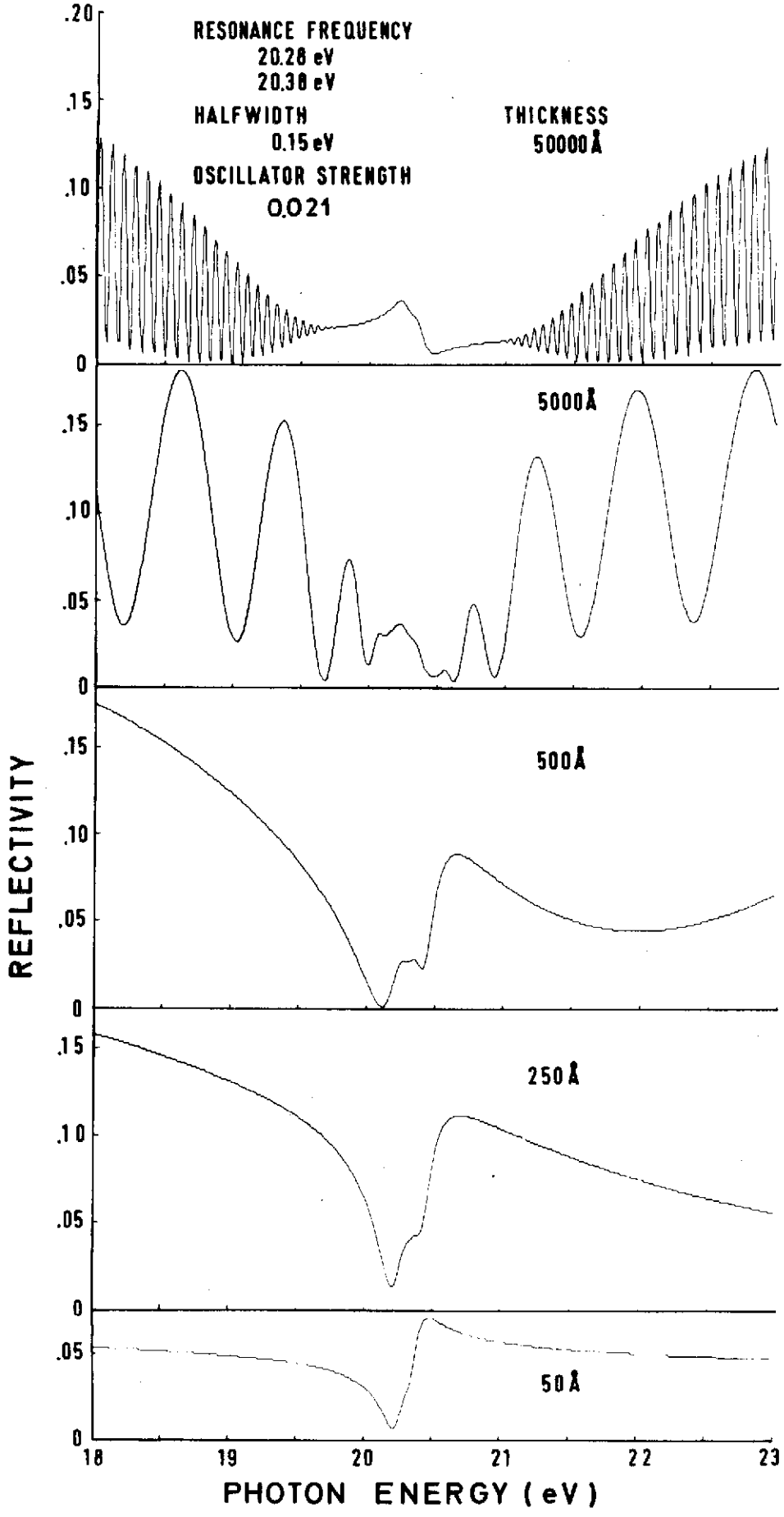
RESONANCE FREQUENCY
20.28 eV
20.38 eV
HALFWIDTH
0.15 eV
OSCILLATOR STRENGTH
0.021
THICKNESS
50000Å
5000Å
500Å
250Å
50Å
REFLECTIVITY
PHOTON ENERGY (eV)
.20
.15
.10
.05
0
18
19
20
21
22
23

Fig. 7

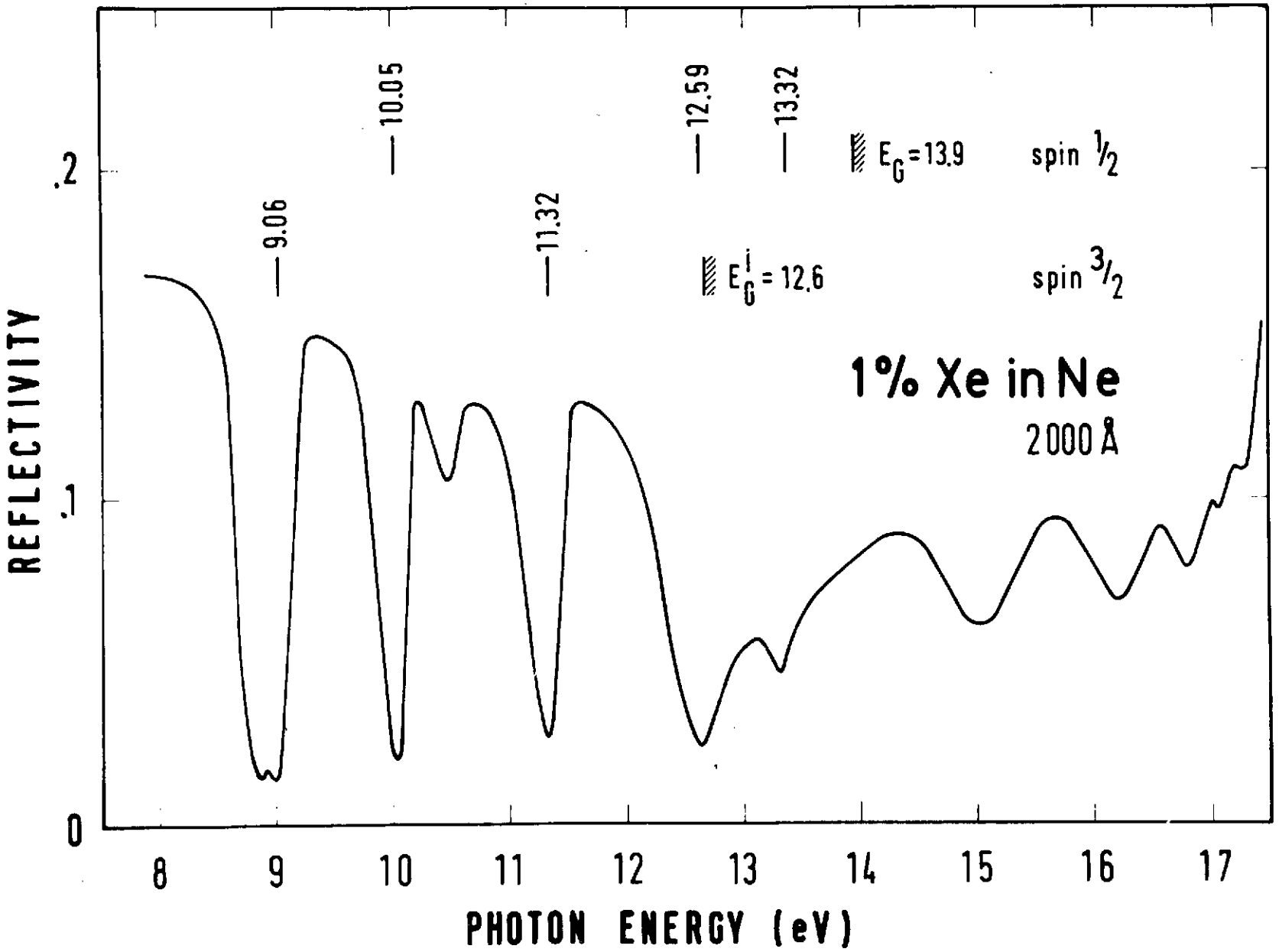
REFLECTIVITY
.2
.1
0
8
9
10
11
12
13
14
15
16
17
PHOTON ENERGY (eV)
9.06
10.05
11.32
12.59
13.32
$E_G = 13.9$ spin 1/2
$E_G^i = 12.6$ spin 3/2
1% Xe in Ne
2000 Å

Fig. 8

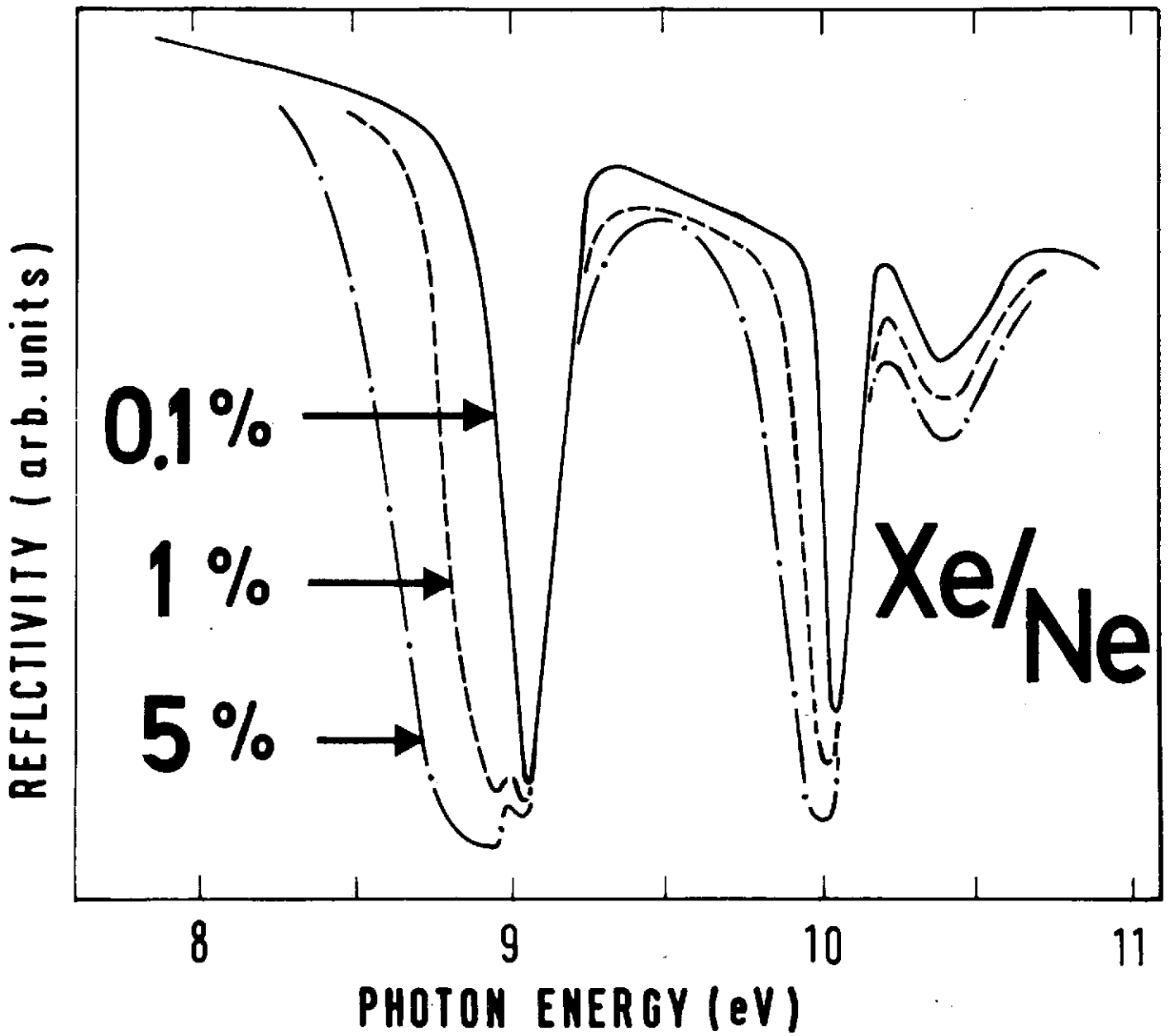

Fig. 9

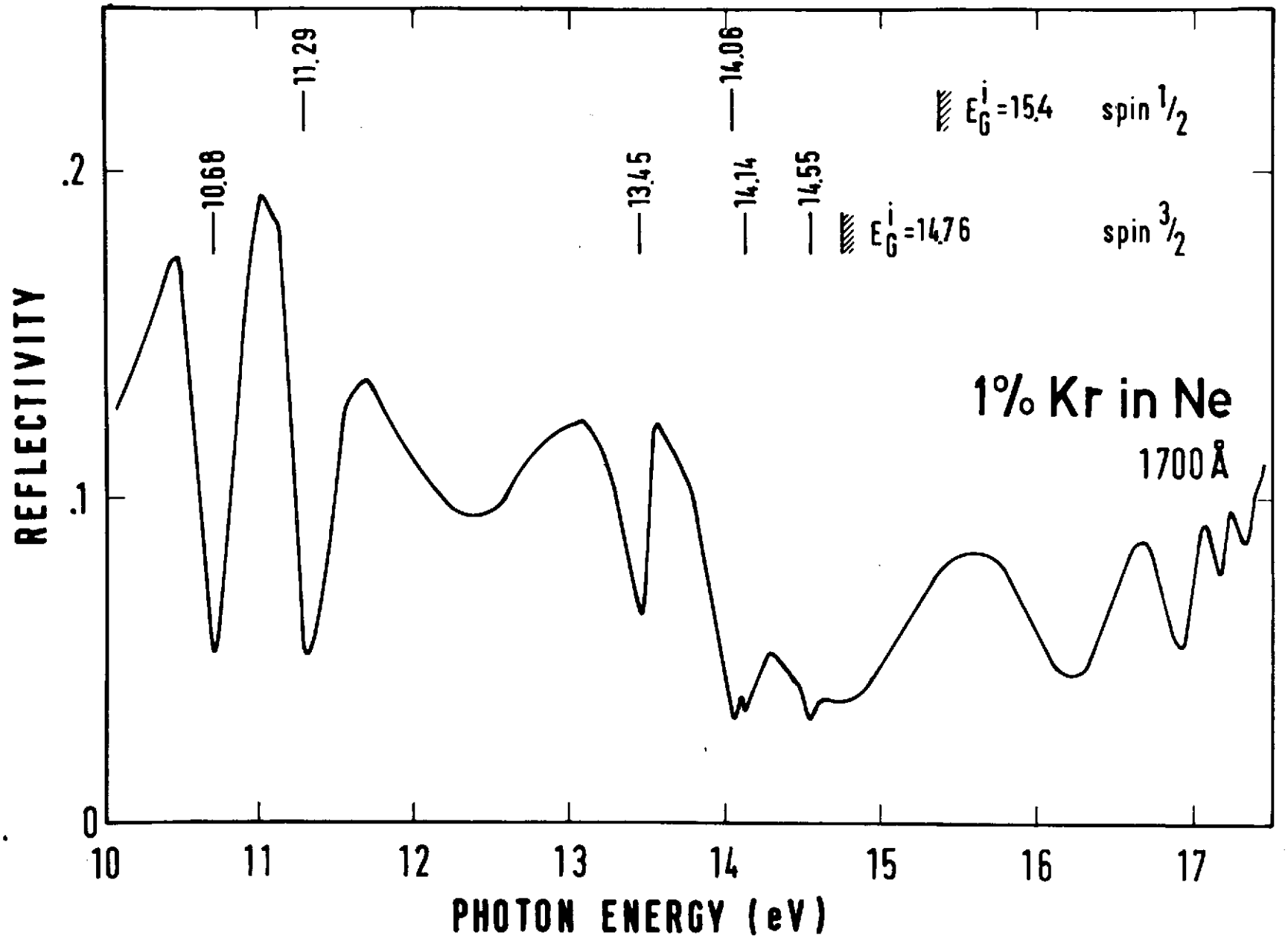
11.29
14.06
E_G^i=15.4
spin 1/2
10.68
13.45
14.14
14.55
E_G^i=14.76
spin 3/2
1% Kr in Ne
1700 Å
REFLECTIVITY
.2
.1
0
10
11
12
13
14
15
16
17
PHOTON ENERGY (eV)

Fig. 10

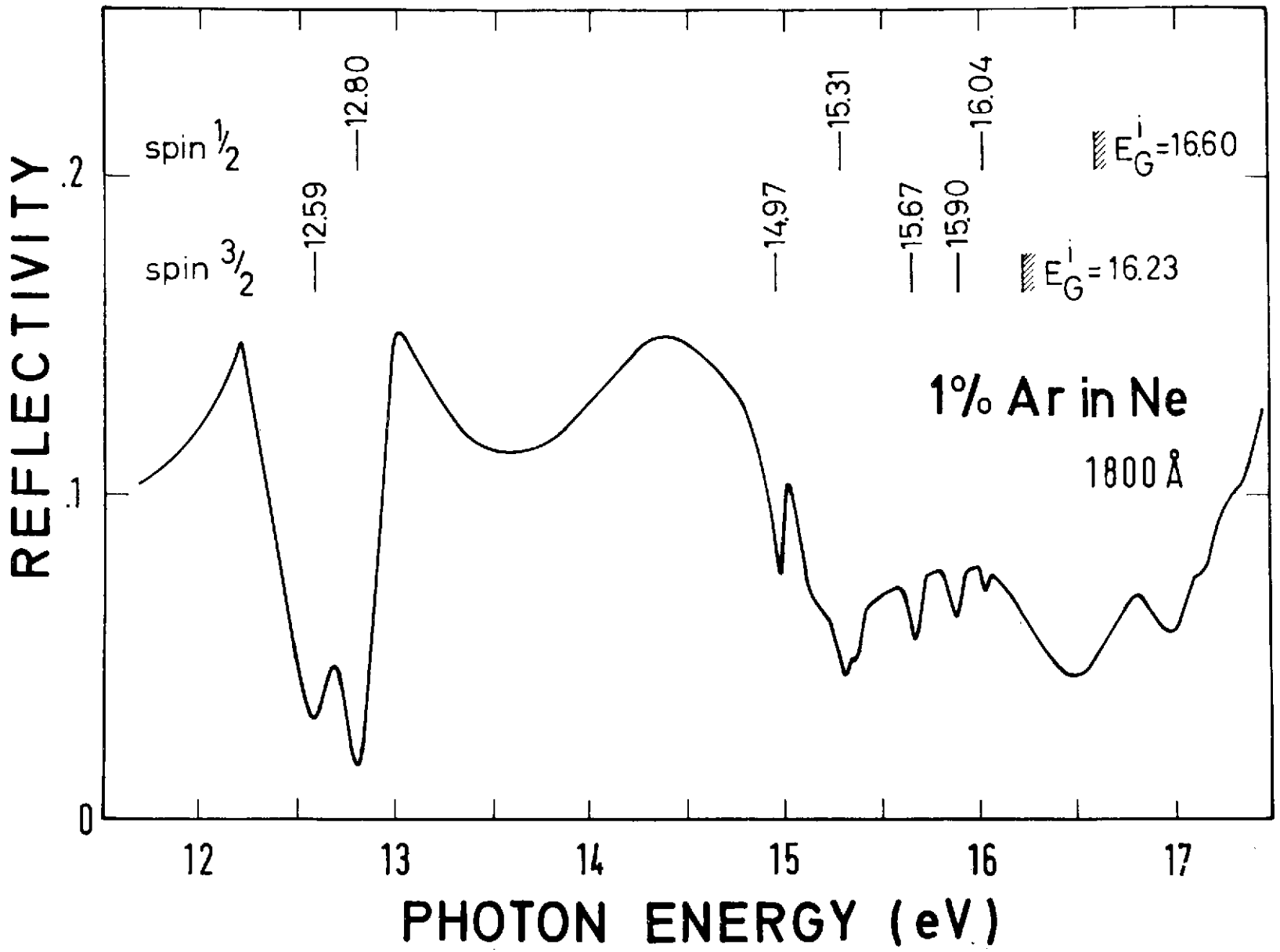
REFLECTIVITY
.2
.1
0
spin 1/2
spin 3/2
12.59
12.80
14.97
15.31
15.67
15.90
16.04
E_G^i=16.60
E_G^i=16.23
1% Ar in Ne
1800 Å
12
13
14
15
16
17
PHOTON ENERGY (eV)

Fig. 11

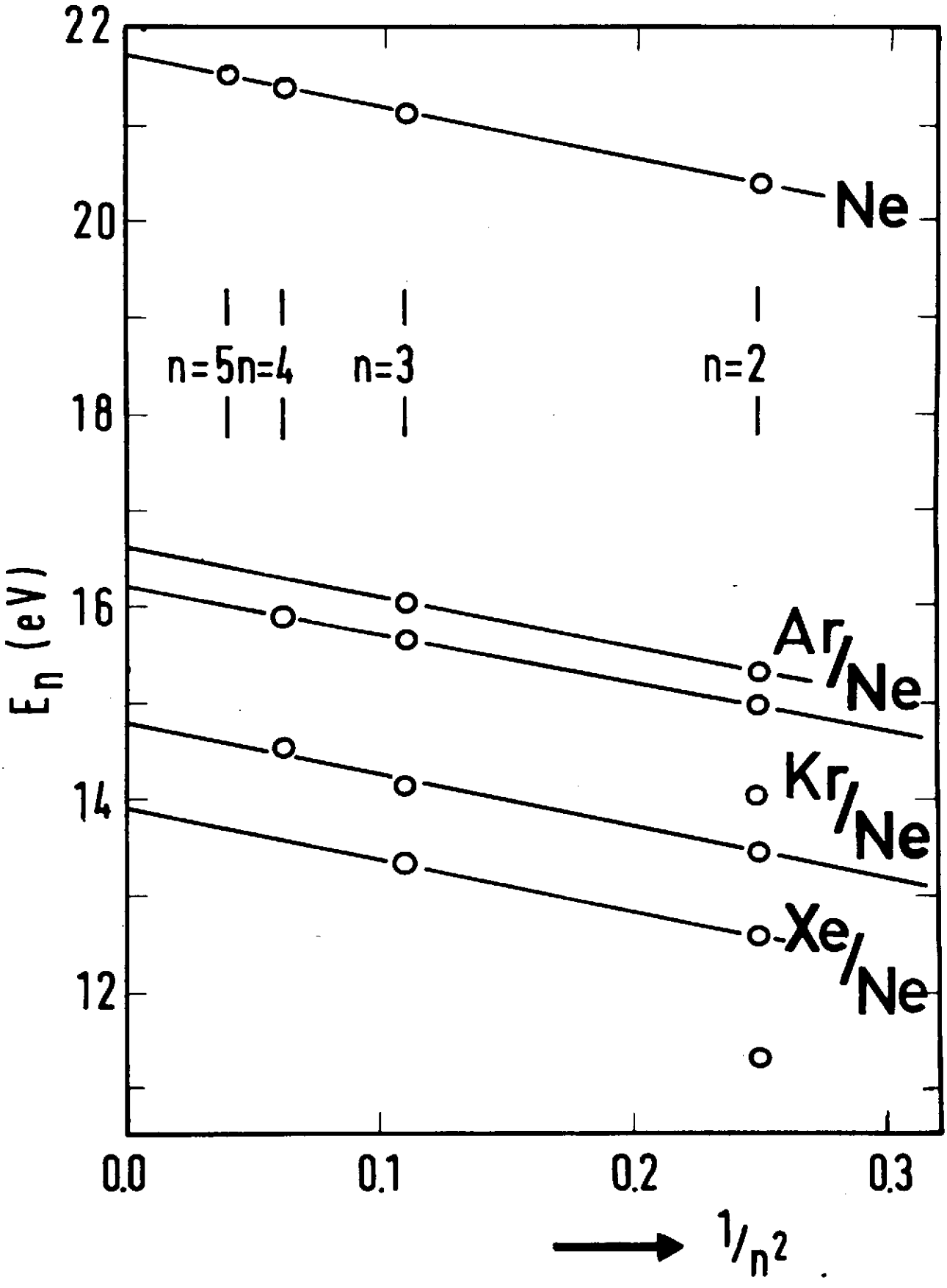

Fig. 12

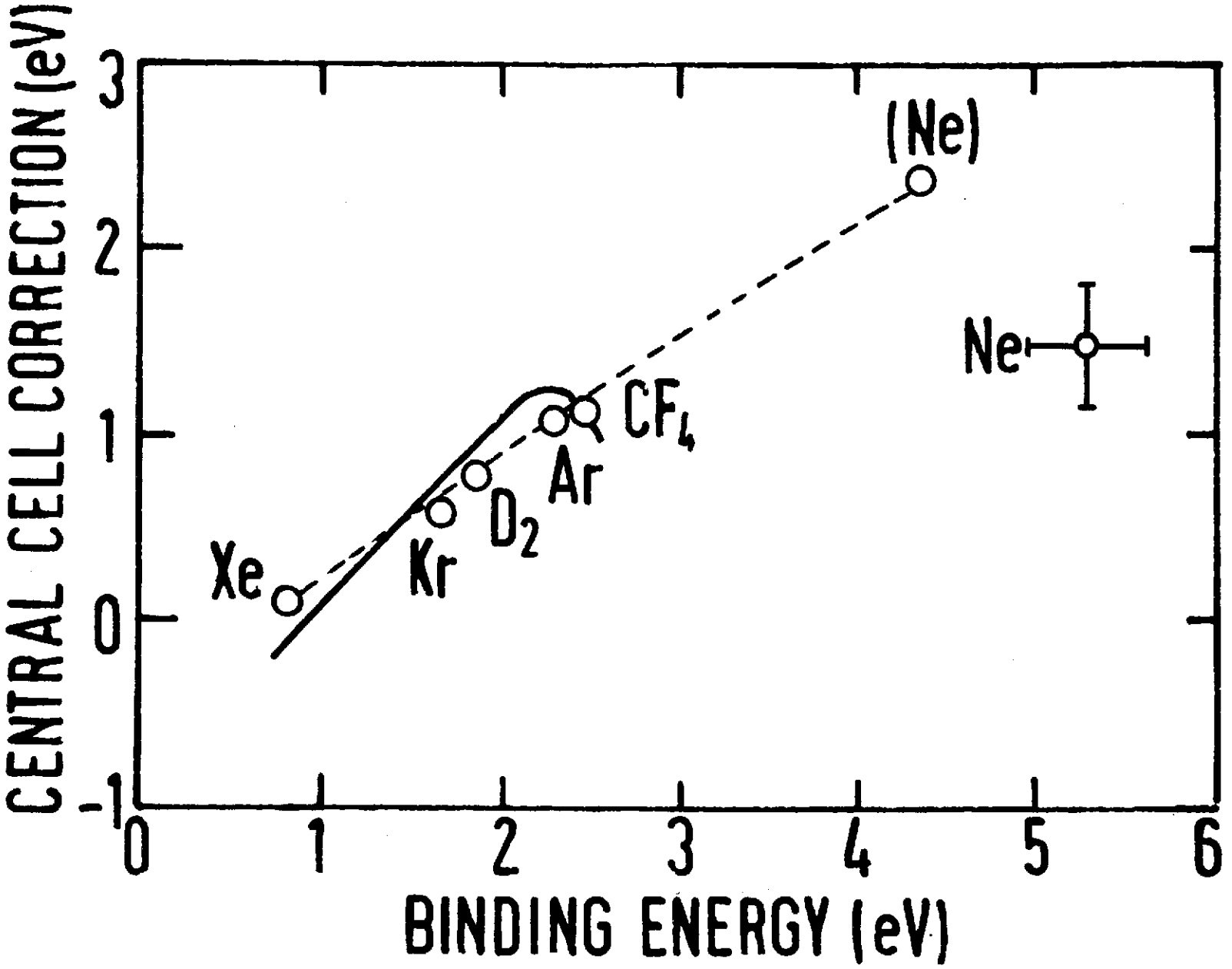
CENTRAL CELL CORRECTION (eV)
3
2
1
0
-1
0
1
2
3
4
5
6
BINDING ENERGY (eV)
(Ne)
Ne
CF4
Ar
D2
Kr
Xe

Fig. 13